Continuous collision detection for composite quadric models

Yi-King Choi [a,*], Wenping Wang [a], Bernard Mourrain [b], Changhe Tu [c], Xiaohong Jia [d], Feng Sun [a]

[a] Department of Computer Science, The University of Hong Kong, Hong Kong
[b] GALAAD, Inria Sophia Antipolis Méditerranée, France
[c] Department of Computer Science and Technology, Shandong University, China
[d] KLMM, AMSS & NCMIS, Chinese Academy of Science, China

ABSTRACT

A composite quadric model (CQM) is an object modeled by piecewise linear or quadric patches. We study the continuous collision detection (CCD) problem of a special type of CQM objects which are commonly used in CAD/CAM, with their boundary surfaces intersect only in straight line segments or conic curve segments. We derive algebraic formulations and compute numerically the first contact time instants and the contact points of two moving CQMs in $\mathbb{R}^3$. Since it is difficult to process CCD of two CQMs in a direct manner because they are composed of semi-algebraic varieties, we break down the problem into subproblems of solving CCD of pairs of boundary elements of the CQMs. We present procedures to solve CCD of different types of boundary element pairs in different dimensions. Some CCD problems are reduced to their equivalents in a lower dimensional setting, where they can be solved more efficiently.

© 2014 Elsevier Inc. All rights reserved.

1. Introduction

Collision detection is important to many fields involving object interaction and simulation, e.g., computer animation, computational physics, virtual reality, robotics, CAD/CAM and virtual manufacturing. Its primary purpose is to determine possible contacts or intersections between objects so that proper responses may be further carried out accordingly. There has been considerable research in relation to collision detection, particularly in the field of robotics and computer graphics, regarding the different issues such as intersection tests, bounding volume computation, and graphics hardware speedup [1,2]. Among these studies, continuous collision detection (CCD) is currently an

active research topic, in which collision status within a continuous time span is determined.

Quadric surfaces form an important class of objects used in practice. In CAD/CAM or industrial manufacturing, objects are often designed and modeled using quadric surfaces because of their simple representations and ease of handling. Quadric surfaces encompass all degree two surfaces, which include the commonly used spheres, ellipsoids, cylinders and cones. Ellipsoids, truncated/capped cylinders and cones are usually used as approximations to complex geometry in graphics and robotics [3,4]. Furthermore, most mechanical parts can be modeled accurately with quadric surfaces. Through composite representation or CSG (constructive solid geometry) composition, an even wider class of complex objects are modeled by quadric surfaces.

Most existing collision detection methods are intended for piecewise linear objects such as triangles, boxes, polyhedrons, or simple curved primitives such as spheres [5–8]. Collision detection of objects containing quadric

* Corresponding author.
   E-mail addresses: ykchoi@cs.hku.hk (Y.-K. Choi), wenping@cs.hku.hk (W. Wang), bernard.mourrain@inria.fr (B. Mourrain), chtu@sdu.edu.cn (C. Tu), xhjia@amss.ac.cn (X. Jia), fsun@cs.hku.hk (F. Sun).

surfaces may be done by applying these methods to piecewise linear approximations of the objects. This, however, introduces geometric error and entails large storage space. As a result, exact collision detection of quadric surfaces is important due to the extensive use of quadric surfaces as modeling primitives in applications.

In this paper we present a framework for efficient and exact continuous collision detection (CCD) of *composite quadric models*, or CQMs for short. CQMs are modeled by piecewise linear or quadric surface patches. The *boundary elements* of a CQM may either be a *face* (a linear or quadric surface patch), an *edge* (where two faces meet) or a *vertex* (where three or more edges meet). A boundary edge of a CQM is in general a degree four intersection curve of two quadrics. However, there is a special class of CQMs whose boundary edges are straight line or conic curve segments only (Fig. 1). In this paper, we focus on CCD of this special class of CQMs (which we shall also denote as "CQM" for brevity), which is by itself an important problem due to the popular use of the class in practice. This work also represents a step towards tackling CCD of general CQMs, which is difficult to be solved efficiently.

Our main contributions are as follows.

- We present a framework for exact and efficient continuous collision detection (CCD) of two moving composite quadric models (CQMs). Given two moving CQMs which are separate initially, our method computes their first contact time and contact point. The CQMs may undergo both the Euclidean and affine motions, which means that the objects may either be rigid or change their shapes under affine transformations.
- Our framework comprises a collection of algebraic methods for CCD of different types of boundary components of a CQM. In particular,
  1. we devise an algorithm for CCD of two moving quadrics (Section 5.1), which is based on our recent result of detecting morphological change of intersection curve for two moving quadrics [9]; and
  2. we derive algebraic conditions for different configurations of 1D conics in $\mathbb{PR}$ and further devise an algorithm for CCD of two moving conics in 3D (Section 5.7).
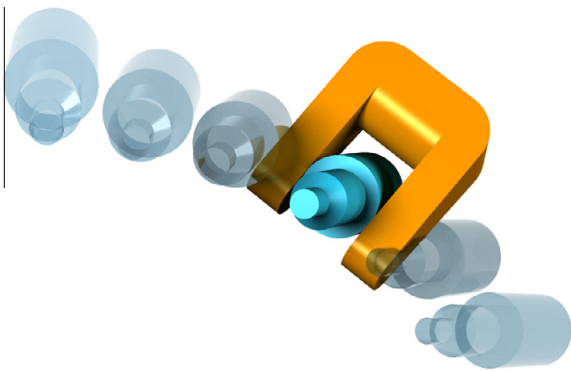

Fig. 1. Two CQMs in motion. The objects are typical examples of the special class of CQMs whose boundary edges are straight line or conics curve segments only.

2. Related work

2.1. Continuous collision detection

Different approaches have been proposed for solving continuous collision detection (CCD) for various types of moving objects. There are CCD methods by equation solving, which include [5,10] for polyhedra, [11] for elliptic disks and [12] for ellipsoids.

Swept volumes (SV) are also commonly used: [13] presents a solution using a four-dimensional space–time SV; [14,15] deal with CCD of articulated bodies by considering SVs of line swept spheres (LSS); and [16] works on SVs of triangles to solve CCD of deformable models with significant speedup using GPU.

Efficiency and accuracy are the major concerns for CCD. Ref. [17] uses the approach of conservative advancement and achieve acceleration of CCD for articulated objects by using the Taylor model which is a generalization of interval arithmetic. For deforming triangle meshes, Ref. [18] proposes conservative local advancement that significantly improve CCD performance by computing motion bounds for the bounding volumes of the primitives. A recent work by [19] uses geometrically exact predicates for efficient and accurate CCD of deforming triangle meshes.

Our CCD method works on exact representations of CQM models and is based on algebraic formulations. For better efficiency, equation solving for obtaining contact time instants and contact points is done numerically.

2.2. Intersection and collision of quadrics

Classifications and computations of the intersections of two general quadrics are thoroughly studied in classical algebraic geometry [20–22] and CAGD [23–29]. These results, however, consider quadrics in the complex or real projective space, and are not applicable to collision detection problems which concern only the real affine or Euclidean space. There is nevertheless an obvious way to detect intersection between stationary quadrics by computing their real intersection curves. Various algorithms have also been proposed (e.g., [30–34]), whose objectives are to classify the topological or geometric structure of the intersection curves and to derive their parametric representations. However, these methods are difficult to extend for collision detection of moving quadrics.

Our previous work in [11,12] presents algorithms for exact CCD of elliptic disks and ellipsoids, based on an algebraic condition for the separation of two ellipsoids established by [35]. Although quadrics are widely used in many applications, CCD of general quadrics has not been addressed in the literature. We propose recently an algebraic method for detecting the morphological change of the intersection curves of two moving quadrics in 3D real projective space [9]. In this paper, we further devise an algorithm for CCD of moving quadrics which is a subproblem of CCD of CQMs. We also develop a framework to solve CCD of CQMs, the more general class of objects composed of piecewise linear or quadric primitives.

3. Outline of algorithm

Two moving CQMs $\mathcal{Q}_A(t)$ and $\mathcal{Q}_B(t)$, where t is a time parameter in the interval $[t_0, t_1]$, are said to be *collision-free*, if the intersection of $\mathcal{Q}_A(t)$ and $\mathcal{Q}_B(t)$ is empty for all $t \in [t_0, t_1]$; otherwise, they are said to *collide*. Two CQMs $\mathcal{Q}_A(t')$ and $\mathcal{Q}_B(t')$ at a particular time instant t' are *in contact* or *touching*, if their boundaries have nonempty intersection while their interiors are disjoint. Given two initially separate CQMs, our goal is to determine whether the CQMs are collision-free or not; if they collide, their first contact time instant in $[t_0, t_1]$ and the contact point will be computed.

We assume that the CQMs undergo arbitrary affine motions which are expressible as continuous functions of the time parameter t, so that the special type of CQM is preserved. Among the various motion types, rational motions are easily handled by CAGD techniques that deal with splines and polynomials. Our method involves root finding, and in the case of rational motions, the functions are polynomials whose roots can be efficiently solved for by these techniques. Moreover, low-degree rational motions are found to be sufficient for modeling smooth motions in most applications and hence further enhance efficiency. See [36] for a thorough discussion of rational motion design. While rational motions are used in our examples, our method is also applicable to other motions, such as helical motions which are transcendental. Numerical solver will then be needed for root finding of these functions.

CQMs can be viewed as semi-algebraic varieties which are defined by multiple polynomial inequalities. Their boundary elements are often finite pieces on a quadric or a conic and hence it is difficult to process CQMs using algebraic methods in a direct manner. To tackle CCD of CQMs, we consider pairwise CCD between the *extended boundary elements* (Fig. 2) which are defined as follows:
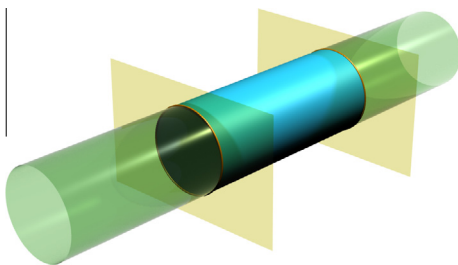
- The complete planar or quadric surface containing a boundary face of a CQM $\mathcal{Q}$ is called an *extended boundary face* of $\mathcal{Q}$.
- The complete straight line or conic curve containing a boundary edge of a CQM $\mathcal{Q}$ is called the *extended boundary edge* of $\mathcal{Q}$.
- An *extended boundary element* of a CQM $\mathcal{Q}$ is either an extended boundary face, an extended boundary edge, or a vertex of $\mathcal{Q}$.

It follows that CCD of CQMs entails solving CCD of different element types. For example, to detect possible contact between two moving capped elliptic cylinders (Fig. 7), one should handle CCD of (a) cylinder vs. cylinder; (b) cylinder vs. ellipse; (c) ellipse vs. plane; and (d) ellipse vs. ellipse.

Our main algorithm is given in Algorithm 1, and the major steps are outlined as follows:

1. Given two CQMs, we first identify CCD subproblems between all possible pairs of their extended boundary elements (Section 4).
2. For each CCD subproblem, we use an algebraic method to compute their first contact instant and point of contact. We will present a classification of different types of CCD problems that one may encounter in CCD of CQMs and discuss the detailed solution to each case (Section 5).
3. Once a contact is found between two extended boundary elements, we will check if the contact is valid, that is, if it lies on both CQMs (Section 6), since a contact found in Step 2 may lie on a portion of an extended boundary element that is not part of a CQM boundary element. Two CQMs are in contact only if the contact point between the extended elements lies on both CQMs (see Fig. 3).
4. After the CCD subproblems are solved, the first valid contact among all pairs of boundary elements is then the first contact of the two CQMs.
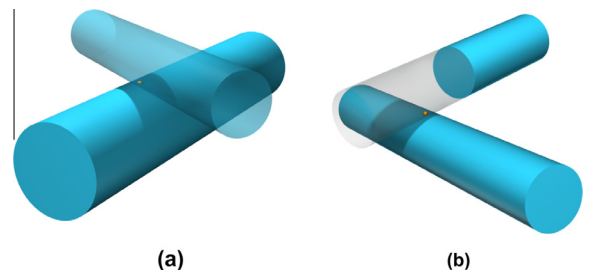

Fig. 2. A capped cylinder (in blue) and its extended boundary elements. The cylinder (in green) and the two planes (in yellow) are the extended boundary elements of the cylindrical surface and the two disks of the capped ends, respectively. The circular edge (in orange) is the extended boundary element of itself. (For interpretation of the references to color in this figure legend, the reader is referred to the web version of this article.)

Fig. 3. Contact validation. (a) The extended boundary elements (cylinders) have a valid contact point that lie on both CQMs, so the capped cylinders are in contact. (b) The contact point of the extended boundary elements is an invalid contact of the CQMs since it does not lie on both CQMs.

Algorithm 1. The Main Algorithm

Input: Two moving CQMs $\mathcal{Q}_A(t)$ and $\mathcal{Q}_B(t)$, $t \in [t_0, t_1]$, and $\mathcal{Q}_A(t_0) \cap \mathcal{Q}_B(t_0) = \emptyset$
Output: Whether $\mathcal{Q}_A(t)$ and $\mathcal{Q}_B(t)$ are collision-free or colliding, and the first contact time and contact point in case of collision

Identify all CCD subproblems between the extended boundary elements of $\mathcal{Q}_A(t)$ and $\mathcal{Q}_B(t)$.
for each CCD subproblem **do**
    Find, if there is any, the first candidate contact time t_i with a valid contact point $\mathbf{p}_i$ that lies on both $\mathcal{Q}_A(t_i)$ and $\mathcal{Q}_B(t_i)$.
    $\mathcal{S} \leftarrow \mathcal{S} \cup \{(t_i, \mathbf{p}_i)\}$
if $\mathcal{S} = \emptyset$ **then**
    return $\mathcal{Q}_A(t)$ and $\mathcal{Q}_B(t)$ is collision-free for $t \in [t_0, t_1]$
else
    $i^* \leftarrow \arg\min\{t_i | (t_i, \mathbf{p}_i) \in \mathcal{S}\}$
    return $(t_{i^*}, \mathbf{p}_{i^*})$ as the first contact time and contact point of $\mathcal{Q}_A(t)$ and $\mathcal{Q}_B(t)$

---

4. Identifying subproblems

A contact of two CQMs always happens between a pair of boundary elements, one from each of the CQMs. In order to detect contact between two CQMs, we define a CCD subproblem for each pair of their extended boundary elements. Depending on the types of the boundary elements, we have different types of contacts—(F, F), (F, E), (F, V), (E, E), (E, V) and (V, V), where F, E and V stand for face, edge and vertex, respectively. However, it suffices to consider only the CCD subproblems of the four basic contact types—(F, F), (F, E), (F, V) and (E, E) to solve CCD of two CQMs, as is shown by the following proposition.

Proposition 1. *A contact between two CQMs can be classified into one of the four basic types:* (F, F), (F, E), (F, V) *and* (E, E).

Proof. A contact between two CQMs can be of more than one contact type, since it may lie on two or more extended boundary elements. Both the (E, V)- and (V, V)-type contacts can be treated as (F, V)-type. In particular, an (E, V)-type contact between a boundary edge E_1 and a vertex V_2 is always also an (F, V)-type contact between V_2 and a boundary face on which E_1 lies. A (V, V)-type contact between two vertices V_1 and V_2 is always also an (F, V)-type contact between V_2 and a boundary face on which V_1 lies. $\square$

5. Solving CCD subproblems

For a pair of extended boundary elements, each from CQMs $\mathcal{Q}_A(t)$ and $\mathcal{Q}_B(t)$, respectively, the next step is to solve their CCD and compute the first contact time instant with the corresponding contact point. There is a hierarchy of extended boundary elements, from faces to vertices, in different dimensions. Each element type also consists of more than one kind of primitives; for instance, a face may either be a quadric face or be a planar face. A complete classification of the types of element pairs that should be considered for CCD of two CQMs is listed in Table 1. In this section, we shall present the techniques for resolving CCD of these cases.

We note here that CCD between two planes can be exempted since any planar face of a CQM must be delimited by some boundary curves and any possible contact of two planes can be found by CCD between one planar face and a boundary curve of another. Similarly, CCD between a plane and a line can also be exempted, since any possible contact between a planar face and a straight edge of two CQMs can be found by CCD between the boundary curve of the face and the line, or CCD between a boundary vertex of the line and the plane. Hence, CCD for these two cases are not listed in Table 1.

5.1. Case I – quadrics vs. quadrics

In this section, we deal with CCD of two quadric surfaces in $\mathbb{R}^3$. We assume that the quadrics are irreducible and hence they do not represent planes. CCD between a quadric surface and a plane is discussed in Section 5.2.

Given two moving quadric surfaces in $\mathbb{R}^3$, our goal is to compute the time instants at which there is a contact

Table 1
Complete classification of different types of element pairs of two CQMs and the technique for solving the corresponding CCD. Note that CCD between two planes and CCD between a plane and a line can be exempted and therefore are not listed here.

Type	Case	Element pairs	Techniques	Section
(F, F)	I	Quadrics vs. Quadrics	CCD of quadrics	5.1
	II	Quadrics vs. Planes	CCD of quadrics/planes	5.2
(F, E)	III	Quadrics vs. Conics	Dimension reduction to Case VIII	5.3
	IV	Planes vs. Conics	Dimension reduction to Case X	5.4
	V	Quadrics vs. Lines	Direct substitution	5.5
(F, V)	VI	Quadrics/Planes vs. Vertices	Direct substitution	5.6
(E, E)	VII	Conics vs. Conics in $\mathbb{R}^3$	Dimension reduction	5.7
	VIII	Conics vs. Conics in $\mathbb{R}^2$	CCD of conics in $\mathbb{R}^2$	5.8
	IX	Conics vs. Lines in $\mathbb{R}^3$	Dimension reduction	5.9
	X	Conics vs. Lines in $\mathbb{R}^2$	Direct substitution	5.10
	XI	Lines vs. Lines	CCD of linear primitives	5.11

between the two quadrics. There are three different local contact configurations between two quadrics: surface contact, curve contact or point contact (Fig. 4). Two quadrics have a *surface contact* if and only if they are identical. They have a *curve contact* if and only if they are tangent at every point along a line or conic curve. There is a *point contact* if and only if they are tangent at an *isolated* common point. It is also important that the quadrics do not intersect locally at the neighborhood of all the tangent points. Fig. 5(a) shows two cylinders that are tangent at a point but also intersect locally at the neigborhood of the same point. The tangent point therefore does not constitute a contact.

Let $X = (x, y, z, w)^T \in \mathbb{PR}^3$ and let two moving quadrics be given by $\mathcal{A}(t) : X^T A(t) X = 0$ and $\mathcal{B}(t) : X^T B(t) X = 0$, where $A(t), B(t)$ are 4×4 matrices with elements as functions in t. The two quadrics define a moving pencil $\mathcal{Q}(\lambda; t) : X^T (\lambda A(t) - B(t)) X = 0$, with characteristic polynomial $f(\lambda; t) = \det(\lambda A(t) - B(t))$. We shall differentiate the cases in which the pencil $\mathcal{Q}(t)$ is (1) in general nondegenerate (i.e., $f(\lambda; t) \not\equiv 0$ for some t), or (2) always degenerate (i.e., $f(\lambda; t) \equiv 0$ for all t), and handle these two cases in different manners to be described in Sections 5.1.1 and 5.1.2, respectively.

5.1.1. For $\mathcal{A}(t)$ and $\mathcal{B}(t)$ whose pencil is in general nondegenerate

In this section, we consider two moving quadrics $\mathcal{A}(t)$ and $\mathcal{B}(t)$ whose pencil is in general nondegenerate, that is, their characteristic polynomial $f(\lambda) = \det(\lambda A(t) - B(t))$ is not always identically zero over the time domain.

The morphologies of the intersection curves of two quadric surfaces (QSICs) in $\mathbb{PR}^3$ have been completely classified in [29]. For two moving quadrics, the morphologies of their QSIC may change over time, and only some QSICs may correspond to a contact between the quadrics. Therefore, our strategy is to first detect the time instants (which we called the *candidate time instants*) at which two moving quadric surfaces have a change in their QSIC. Our next step is then to identify whether a QSIC corresponds to a real contact (face, line or point contact) in $\mathbb{R}^3$ at each of the candidate time instants and to compute the contact between the two quadrics.

5.1.1.1. Determining candidate contact time instants.
The candidate time instants are the moments at which the QSIC of two moving quadrics change its morphological type. To determine the candidate time instants, we make use of our recent result in detecting the variations of the QSIC of two moving quadrics in $\mathbb{PR}^3$. Here, we give a brief idea of how
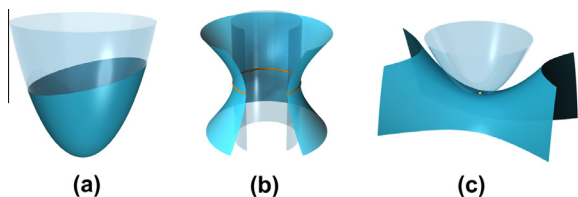

Fig. 4. The three different local contact configurations between two quadrics: (a) surface contact; (b) curve contact; and (c) point contact.
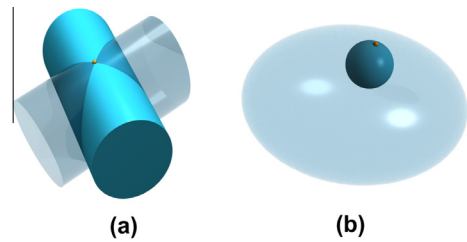

Fig. 5. (a) Two cylinders intersect locally at the neighborhood of the tangent point. (b) There is no local intersection between two ellipsoids at the isolated tangent point. Hence, the ellipsoids in (b) are in contact while the cylinders in (a) are not.

this can be done and refer the reader to [9] for the details. The classification by [29] distinguishes the QSIC types of two quadrics in $\mathbb{PR}^3$ from both algebraic and topological points of view (including singularities, number of components, and the degree of each irreducible component). A QSIC type can be identified by the signature sequence and the Segre characteristics [20] of the quadric pencil $Q(\lambda; t) = \lambda A(t) - B(t)$, which characterize the algebraic properties of the roots of characteristic polynomial of $Q(\lambda; t)$, such as the number of real roots, the multiplicity of each root, and the type of the Jordan blocks associated with each root. We proved that to detect all the time instants at which the QSIC changes is equivalent to detecting the time instants when the Segre characteristic of $Q(\lambda; t)$ changes. This leads to an algebraic method using the techniques of resultants and Jordan forms to compute all the required time instants, which, in our case, will serve as the candidate time instants for the next step.
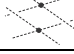
Remark 2. With the aforementioned algebraic method, we obtain univariate equations defining the candidate time instants. The positive real solutions of such univariate equations can be computed efficiently by real root isolation solvers. Checking the sign of a polynomial expression at such a root can be done exactly by algebraic methods (see for example [37]).
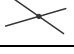
5.1.1.2. Identifying real contact.
For each of the candidate contact time instants t_i, the next step is to determine whether the QSIC corresponds to any real contact between the quadrics $\mathcal{A}(t_i)$ and $\mathcal{B}(t_i)$. Table 2 is adapted from the three classification tables in [29] by showing only those cases[1] in which the QSIC of two distinct quadrics corresponds to a point or a curve contact in $\mathbb{PR}^3$. It therefore encompasses all possible contact configurations of two quadrics. The case of a face contact, that is, the two quadrics being identical, can be trivially identified and is skipped here. Now, for each candidate time instant t_i, we compute the signature sequence of $\mathcal{A}(t_i)$ and $\mathcal{B}(t_i)$ which involves determining the multiplicity of a real root and the signature of a quadric pencil at the root, and can be done

---

[1] We keep the original case numbers for ease of reference.

Table 2

QSIC corresponding to a point contact or curve contact between two distinct quadrics in $\mathbb{PR}^3$ [29]. In the illustrations, a solid line or curve represents a real component while a dashed one represents an imaginary component. A solid dot indicates a real singular point. A null-homotopic component is drawn as a closed loop, and a non-null-homotopic component is shown as an open-ended curve. A line or curve that is counted twice is thickened.

$[\text{Segre}]_r$ r: # real roots	Case #: Index sequence/signature sequence	Illustration	Representative quadric pair
$[211]_3$	**6**: $\langle 1\,\wr\wr_-1|2|3\rangle/(1,\,((1,2)),1,\,(1,2),2,\,(2,1),3)$		$-x^2 - z^2 + 2yw = 0$ $-3x^2 + y^2 - z^2 = 0$
	7: $\langle 1\,\wr\wr_+1|2|3\rangle\ (1,\,((0,3)),1,\,(1,2),2,\,(2,1),3)$		$x^2 + z^2 + 2yw = 0$ $3x^2 + y^2 + z^2 = 0$
$[(11)11]_3$	**15**: $\langle 1||1|2|3\rangle\ (1,\,((0,2)),1,\,(1,2),2,\,(2,1),3)$		$x^2 + y^2 + z^2 - w^2 = 0$ $x^2 + 2y^2 = 0$
$[(111)1]_2$	**19**: $\langle 1|||2|3\rangle\ (1,\,(((0,1))),2,\,(2,1),3)$		$y^2 + z^2 - w^2 = 0$ $x^2 = 0$
$[(21)1]_2$	**22**: $\langle 1\,\wr\wr_+|2|3\rangle\ (1,\,(((0,2))),2,\,(2,1),3)$		$y^2 - z^2 + 2zw = 0$ $x^2 + z^2 = 0$
$[2(11)]_2$	**24**: $\langle 1\,\wr\wr_-1||3\rangle\ (1,\,((1,2)),1,\,((1,1)),3)$		$2xy - y^2 = 0$ $y^2 - z^2 - w^2 = 0$
	25: $\langle 1\,\wr\wr_+1||3\rangle\ (1,\,((0,3)),1,\,((1,1)),3)$		$2xy - y^2 = 0$ $y^2 + z^2 + w^2 = 0$
$[(11)(11)]_2$	**30**: $\langle 1||1||3\rangle\ (1,\,((0,2)),1,\,((1,1)),3)$		$x^2 + y^2 = 0$ $z^2 - w^2 = 0$
$[(211)]_1$	**32**: $\langle 2\,\wr\wr_-||2\rangle\ (2,\,((((1,0)))),2)$		$x^2 - y^2 + 2zw = 0$ $z^2 = 0$
	33: $\langle 1\,\wr\wr_-||3\rangle\ (1,\,((((1,0)))),3)$		$x^2 + y^2 + 2zw = 0$ $z^2 = 0$
$[(22)]_1$	**34**: $\langle 2\widehat{\wr}_-\widehat{\wr}_-2\rangle\ (2,\,((((2,0)))),2)$		$xy + zw = 0$ $y^2 + w^2 = 0$
	35: $\langle 2\widehat{\wr}_-\widehat{\wr}_+2\rangle\ (2,\,((((1,1)))),2)$		$xy - zw = 0$ $y^2 - w^2 = 0$

using rational arithmetic.[2] The quadrics have a contact in $\mathbb{PR}^3$ if and only if the sequence matches one of the 12 cases listed in Table 2. The following example shows how we may identify if two quadrics have a contact at a particular time instant by checking their Segre characteristics and signature sequence against Table 2.

Example 3. Consider two cylinders, $\mathcal{A} : x^2 + z^2 = 1$ and $\mathcal{B} : y^2 + z^2 = 1$, which have two singular intersection points as shown in Fig. 5(a). The characteristic equation is $f(\lambda) = \lambda(\lambda - 1)^2 = 0$. The Segre characteristics and the signature sequence are found to be $[(11)11]_3$ and $(2,\,((1,1)),2,\,(1,2),1,\,(1,2),2)$, respectively, which corresponds to case 13 of [29] in which the QSIC has two conics intersecting at two distinct non-isolated singular points. This case does not correspond to a contact configuration

and is not listed in Table 2. The two cylinders are therefore not in contact.

5.1.1.3. Computing contact. We can proceed to compute a contact once it is identified. The following lemma provides a means to computing the contact points of two quadrics at a particular time instant:

Lemma 4. *Let $\mathcal{A} : X^T A X = 0$ and $\mathcal{B} : X^T B X = 0$ be two distinct, irreducible quadric surfaces whose pencil is nondegenerate. Suppose that $\mathcal{A}$ and $\mathcal{B}$ are in contact (i.e., whose QSIC is listed in Table 2), and let λ_0 be a multiple root of $f(\lambda) = \det(\lambda A - B) = 0$, the characteristic equation of $\mathcal{A}$ and $\mathcal{B}$. Then, we have the following cases:*

1. *If $\text{rank}(\lambda_0 A - B) = 3$, λ_0 corresponds to one singular intersection point $\mathbf{p}$ of $\mathcal{A}$ and $\mathcal{B}$ in $\mathbb{PR}^3$. If $\lambda_0 \neq 0$, $\mathcal{A}$ and $\mathcal{B}$ are tangential at $\mathbf{p}$; otherwise, $\mathcal{B}$ is a cone with $\mathbf{p}$ as its apex which lies also on $\mathcal{A}$.*
2. *If $\text{rank}(\lambda_0 A - B) = 2$, λ_0 corresponds to singular intersection between $\mathcal{A}$ and $\mathcal{B}$ that happens at either one point, two distinct points, or along a straight line in $\mathbb{PC}^3$, where $\mathcal{A}$ and $\mathcal{B}$ are tangential to each other.*

3. If $rank(\lambda_0 A - B) = 1$, λ_0 corresponds to singular intersection between $\mathcal{A}$ and $\mathcal{B}$ along a conic curve (which can be a reducible one) in $\mathbb{PC}^3$, where $\mathcal{A}$ and $\mathcal{B}$ are tangential to each other.

The proof can be found in [38].

Note that when $f(\lambda) = 0$ has more than one multiple root, we should consider all its multiple roots in order to obtain all contact points between the two quadrics. According to Lemma 4, given two touching quadric surfaces at time t_i, the contact points are in general the solutions of $(\lambda_j A(t_i) - B(t_i))X = 0$ for each multiple root λ_j of $f(\lambda; t_i) = 0$. We also need to differentiate between real and imaginary contacts. For example in both cases 24 and 25 of Table 2, the characteristic equation has two multiple roots λ_0 and λ_1, with $rank(\lambda_0 A - B) = 3$ and $rank(\lambda_1 A - B) = 2$; λ_0 corresponds to a real contact point while λ_1 corresponds to two distinct imaginary contacts which should be discarded.

Example 5. Consider the unit sphere $\mathcal{A} : x^2 + y^2 + z^2 = 1$ and a cylinder $\mathcal{B} : x^2 + y^2 = 1$. The characteristic equation of $\mathcal{A}$ and $\mathcal{B}$ is $f(\lambda) = -\lambda(\lambda - 1)^3$ which has a triple root $\lambda_0 = 1$. Also, $rank(\lambda_0 A - B) = 1$ and by Lemma 4, λ_0 corresponds to a contact along a conic curve between $\mathcal{A}$ and $\mathcal{B}$. Now, $(\lambda_0 A - B)X = 0$ has three linearly independent solutions $X_0 = (0, 0, 0, 1)^T$, $X_1 = (1, 0, 0, 0)^T$ and $X_2 = (0, 1, 0, 0)^T$ which span the plane $z = 0$. Intersecting the plane $z = 0$ with $\mathcal{A}$ yields the circle $x^2 + y^2 = 1, z = 0$, which is the contact between $\mathcal{A}$ and $\mathcal{B}$.

Cases 6, 24 and 35 are situations in which the quadrics are tangent at some regions but at the same time having local real intersection at the others. Since we assume that the CQMs are separate initially and we seek their first contact, it can be assured that a local real intersection must take place after a proper contact is found. The real intersections in these cases can therefore be ignored.

The contact points computed so far are between the quadric surfaces but not necessarily between the CQMs, therefore all contact points are further subject to validation to see if they are on both CQMs. Contact points at infinity are thus discarded. Validation details will be discussed in Section 6.

5.1.2. For $\mathcal{A}(t)$ and $\mathcal{B}(t)$ whose pencil is always degenerate

We now consider the case of two moving quadrics which always define a degenerate pencil, that is, $f(\lambda; t) \equiv 0$ for all t. Here, all members of the pencils are projective cones for all t [39], which means that the vertices of the projective cones always lie on a common generator of the cones and the cones are always tangential along this generator in $\mathbb{PC}^3$. Considering any affine realization of the projective space, Fig. 6 depicts the three situations of this kind that are only possible in $\mathbb{R}^3$: (a) Two moving cones whose apexes slide along the common generator, (b) two moving cylinders whose axes are always parallel (with their "apexes" at infinity), and (c) a moving cone and a moving cylinder which always share a common generator. Note that a cylinder can either be an elliptic, a hyperbolic or a parabolic cylinder. For case (a), we need
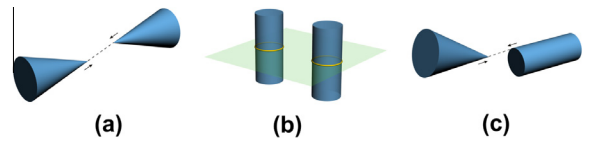

Fig. 6. The three possible scenarios of two moving quadrics in $\mathbb{R}^3$ whose pencil is always degenerate. (a) Two moving cones whose vertices always lie on a common generator; (b) two moving cylinders whose axes are always parallel; and (c) a moving cone and a moving cylinder which always share a common generator. Note that a cylinder may either be an elliptic, a hyperbolic or a parabolic cylinder. Also, only one nappe of a cone is shown.

only to consider the contact of the vertices, since the cones are initially separate and any other contact configurations can be detected by CCD of other boundary elements of the CQMs. Hence, the candidate contact time instants are the contact time instants of the vertices of the cones. For (b), the CCD problem is transformed to a two-dimensional CCD of two moving conics on a plane $\mathcal{P}$ orthogonal to the cylinder axes, with the conics being the cross-sections of the cylinders on $\mathcal{P}$. CCD of moving conics in $\mathbb{R}^2$ will be discussed in Section 5.8. We may disregard case (c) for a moving cone and a moving cylinder, since a cylinder must be delimited by a boundary curve on a CQM and any possible first contact can be captured by CCD of other boundary elements of the CQMs.

5.2. Case II – quadrics vs. planes

We first note that the singular case where a plane is in contact with a cone only at its apex is not considered here, as the contact can be determined directly by an (F, V)-type CCD of the apex and the plane.

Now, consider an irreducible quadric surface $\mathcal{A}(t) : X^T A(t)X = 0$ and a plane $\mathcal{N}(t) : N(t)^T X = 0$ in $\mathbb{R}^3$. A necessary and sufficient condition for $\mathcal{N}(t)$ to be a tangent plane to $\mathcal{A}(t)$ at some point $X_0 \in \mathbb{R}^3$ is that

$$\begin{cases} \alpha N(t) = A(t)X_0 & \text{for some nonzero } \alpha \in \mathbb{R}, \text{ and} \\ N(t)^T X_0 = 0. \end{cases}$$

These two equations can be written as

$$\begin{pmatrix} A(t) & N(t) \\ N(t)^T & 0 \end{pmatrix} \begin{pmatrix} X_0 \\ -\alpha \end{pmatrix} = 0,$$

which has a nonzero solution $(X_0\ \alpha)^T$ if

$$\begin{vmatrix} A(t) & N(t) \\ N(t)^T & 0 \end{vmatrix} = 0. \tag{1}$$

Therefore, the roots of Eq. (1) corresponding to a solution $(X_0\ \alpha)^T$ with $\alpha \neq 0$ yield the candidate time instants of the quadric $\mathcal{A}(t)$ and the plane $\mathcal{N}(t)$.

5.3. Case III – quadrics vs. conics

We adopt a *dimension reduction technique* to reduce CCD of extended boundary elements to CCD of primitives of lower dimensions. By doing so, we also simplify the
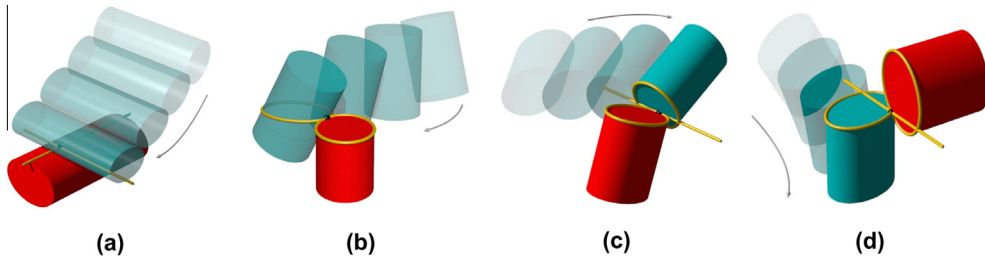
Fig. 7. Contact configurations of two capped cylinders determined by CCDs of four different types of element pair. (a) (F, F)-type; (b & c) (F, E)-type; and (d) (E, E)-type. CCDs of (b)–(d) are solved using the dimension reduction technique.

algebraic formulations. Fig. 7 illustrates CCD of two moving capped elliptic cylinders. In this example, there are three cases to which the dimension reduction technique can be applied, namely, quadrics vs. conics (Fig. 7(b)), planes vs. conics (Fig. 7) and conics vs. conics (Fig. 7(d)). The reduction for the latter two cases will be discussed in subsequent sections.

We first consider CCD of a quadric surface $\mathcal{S}(t) : X^T S(t) X = 0$ and a conic curve $\mathcal{C}(t)$ defined in the plane $\Pi_{\mathcal{C}}(t)$ in $\mathbb{R}^3$. Let $\mathcal{S}_\Pi(t)$ be the intersection of $\mathcal{S}(t)$ with $\Pi_{\mathcal{C}}(t)$. We thereby reduce CCD of $\mathcal{S}(t)$ and $\mathcal{C}(t)$ to CCD of $\mathcal{S}_\Pi(t)$ and $\mathcal{C}(t)$, which are two conics, in the plane $\Pi_{\mathcal{C}}(t)$. CCD of two conics in $\mathbb{R}^2$ is handled in Case VIII (Section 5.8).

5.4. Case IV – planes vs. conics

Consider CCD of a plane $\mathcal{P}(t)$ and a conic curve $\mathcal{C}(t)$ defined in a plane $\Pi_{\mathcal{C}}(t)$ in $\mathbb{R}^3$. The case of $\mathcal{P}(t)$ and $\Pi_{\mathcal{C}}(t)$ being identical for all t can be disregarded, as any possible first contact of the CQMs due to $\mathcal{P}(t)$ and $\mathcal{C}(t)$ can then be detected by CCD of $\mathcal{C}(t)$ and other boundary elements on $\mathcal{P}(t)$. If $\mathcal{P}(t)$ and $\Pi_{\mathcal{C}}(t)$ are parallel for all t, then there is no contact between $\mathcal{P}(t)$ and $\mathcal{C}(t)$. Otherwise, with dimension reduction, CCD of a plane $\mathcal{P}(t)$ and a conic curve $\mathcal{C}(t)$ is reduced to CCD of $\mathcal{C}(t)$ and a moving line which is the intersection between $\mathcal{P}(t)$ and $\Pi_{\mathcal{C}}(t)$ in $\mathbb{R}^2$, and the latter is handled by Case X (Section 5.10) for CCD between conics and lines in $\mathbb{R}^2$. For the candidate time instants thus found, we will verify and discard those t_i at which $\mathcal{P}(t_i)$ and $\Pi_{\mathcal{C}}(t_i)$ are parallel.

5.5. Case V – quadrics vs. lines

Suppose $\mathcal{S}(t) : X^T S(t) X = 0$ is a quadric surface and $\mathcal{L}(u; t)$ is a line in $\mathbb{R}^3$. We simply substitute $\mathcal{L}(u; t)$ into $\mathcal{S}(t)$ and obtain $g(u; t) = L(u; t)^T S(t) L(u; t)$ which is quadratic in u. The line $\mathcal{L}(u; t_i)$ touches $\mathcal{S}(t_i)$ at a particular time t_i if $g(u; t_i)$ has a double root u_0. Hence, the candidate contact time instants of $\mathcal{S}(t)$ and $\mathcal{L}(u; t)$ are given by the roots of the discriminant Δ_g of $g(u; t)$. For each candidate contact time instant t_i, the contact point is $\mathcal{L}(u_0; t_i)$ where u_0 is the double root of $g(u; t_i)$. If $g(u; t_i)$ is identically zero, we have $\mathcal{L}(u; t_i)$ lying entirely on $\mathcal{S}(t_i)$.

5.6. Case VI – quadrics/planes vs. vertices

Let $\mathcal{S}(t) : X^T S(t) X = 0$ be a quadric surface and $\mathbf{p}(t)$ be a vertex in $\mathbb{R}^3$. By direct substitution, we obtain the equation $\mathbf{p}^T(t) S(t) \mathbf{p}(t) = 0$ whose roots give the candidate contact time instants. Similarly, for CCD of a plane $\mathcal{H}(t) : H(t)^T X = 0$ and a vertex $\mathbf{p}(t)$, the candidate contact time instants are the roots of the equation $H(t)^T \mathbf{p}(t) = 0$.

5.7. Case VII – conics vs. conics in $\mathbb{R}^3$

We transform the problem of CCD of two conics in $\mathbb{R}^3$ into CCD of one dimension in the line where the containing planes of the conics intersect. Let a moving conic $\mathcal{A}(t)$ be defined as the intersection between a quadric $\widetilde{\mathcal{A}}(t) : X^T A(t) X = 0$ and a plane $\Pi_A(t)$ in $\mathbb{R}^3$. Similarly, $\mathcal{B}(t)$ is a moving conic which is the intersection between a quadric $\widetilde{\mathcal{B}}(t) : X^T B(t) X = 0$ and a plane $\Pi_B(t)$ in $\mathbb{R}^3$. We first assume that $\Pi_A(t) \not\equiv \Pi_B(t)$ and let $\mathcal{L}(u; t)$ be a parameterization of the line of intersection between $\Pi_A(t)$ and $\Pi_B(t)$.

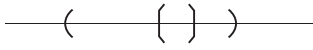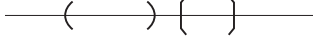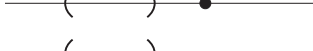Substituting $\mathcal{L}(u; t)$ into the conic equations, we have:
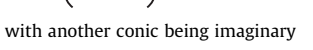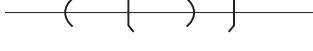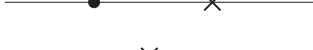
$$h(u; t) : \ L^T(u; t) A(t) L(u; t) = 0, \qquad (2)$$
$$g(u; t) : \ L^T(u; t) B(t) L(u; t) = 0.$$

The solution of $h(u; t) = 0$ gives the intersection between $\mathcal{L}(u; t)$ and $\mathcal{A}(t)$. Likewise, the solution of $g(u; t) = 0$ gives the intersection between $\mathcal{L}(u; t)$ and $\mathcal{B}(t)$. Since $h(u; t)$ and $g(u; t)$ are quadratic in u, we may write $h(u; t) = U^T \widehat{A}(t) U$ and $g(u; t) = U^T \widehat{B}(t) U$ where $U = (u, 1)^T$ and $\widehat{A}(t)$ and $\widehat{B}(t)$ are 2×2 coefficient matrices. It means that $h(u; t)$ and $g(u; t)$ can be considered as two moving "1D projective conics" (i.e., intervals or line segments), denoted by $\widehat{\mathcal{A}}(t)$ and $\widehat{\mathcal{B}}(t)$, which can be either real or imaginary. Now, $\mathcal{A}(t)$ and $\mathcal{B}(t)$ have real tangency in $\mathbb{PR}^3$ if and only if there is real tangency between $\widehat{\mathcal{A}}(t)$ and $\widehat{\mathcal{B}}(t)$ in $\mathbb{PR}^3$, that is, an end-point of $\widehat{\mathcal{A}}(t)$ overlap with an end-point of $\widehat{\mathcal{B}}(t)$. Hence, we have essentially reduced a 3D problem (namely, CCD of two moving conics in the space) to a 1D problem (namely, CCD of two moving intervals in a line).

Let $f(\lambda) = \det(\lambda \widehat{A} - \widehat{B})$ be the characteristic polynomial of two static 1D conics $\widehat{\mathcal{A}} : X^T \widehat{A} X = 0$ and $\widehat{\mathcal{B}} : X^T \widehat{B} X = 0$ in $\mathbb{PR}$. The intersection of $\widehat{\mathcal{A}}$ and $\widehat{\mathcal{B}}$ can be characterized by the roots of $f(\lambda)$, as summarized in Table 3 (the derivation follows similarly as in [40] for the characterization of the intersection of two 1D ellipses in $\mathbb{R}$). Hence, we have the

Table 3

Configuration of two 1D conics $\widehat{\mathcal{A}}$ & $\widehat{\mathcal{B}}$ in $\mathbb{PR}$ and the roots of their characteristic equation $f(\lambda) = 0$. Each 1D conic is represented in pairs of brackets of the same style. Degenerate conic of one point is represented by either a dot or a cross.

Roots of $f(\lambda) = 0$	Configuration
(1) Distinct positive	
	or both $\widehat{\mathcal{A}}$ & $\widehat{\mathcal{B}}$ are imaginary and $\widehat{\mathcal{A}} \neq \widehat{\mathcal{B}}$
(2) Distinct negative	
(3) One zero, one positive	
(4) One zero, one negative	
(5) One negative, one positive	with another conic being imaginary
(6) Positive double	
	or both $\widehat{\mathcal{A}}$ & $\widehat{\mathcal{B}}$ are imaginary and $\widehat{\mathcal{A}} = \widehat{\mathcal{B}}$
(7) Negative double	
(8) Double zero	
(9) Complex conjugate	
(10) $f(\lambda)$ is linear with roots = 0	
(11) $f(\lambda) \equiv 0$	

following theorem stating the conditions for two conics to have contact in $\mathbb{PR}^3$:

Theorem 6. *Given two conics $\mathcal{A}$ (on plane Π_A) and $\mathcal{B}$ (on plane Π_B) in $\mathbb{R}^3$, suppose that Π_A and Π_B intersect at some line $\mathcal{L} \in \mathbb{R}^3$. Let $\widehat{\mathcal{A}} : X^T\widehat{A}X = 0$ and $\widehat{\mathcal{B}} : X^T\widehat{B}X = 0$ be the "1D conics" characterizing the intersections of $\mathcal{L}$ with $\mathcal{A}$ and $\mathcal{B}$, respectively. Furthermore, let $f(\lambda) = \det(\lambda\widehat{A} - \widehat{B})$ be the characteristic polynomial of $\widehat{\mathcal{A}}$ and $\widehat{\mathcal{B}}$. Then, the conics $\mathcal{A}$ and $\mathcal{B}$ are in contact in $\mathbb{PR}^3$ if and only if*

1. *$f(\lambda)$ has a double root (Fig. 8(a-c)); or*
2. *$f(\lambda) \equiv 0$ (Fig. 8(d)).*

Algorithm 2 gives the procedure for solving CCD of two moving conics in $\mathbb{R}^3$. First of all, if two moving conics are found to be contained in the same plane (i.e., $\Pi_A(t) \equiv \Pi_B(t)$) for all t, we may apply a continuous transformation $M(t)$ to both conics that maps $\Pi_A(t)$ to $\mathbb{R}^2$ and the problem is reduced to a two dimensional CCD of two moving conics in $\mathbb{R}^2$. Otherwise, we reduce the problem to a one dimensional CCD of two 1D conics using the above formulation and capture the time instants at which the conditions in Theorem 6 are satisfied. This is done by computing the zeroes of the discriminant $\Delta_f(t)$ of $f(\lambda; t)$ which give the instants t_i when $f(\lambda; t_i)$ has a double root (condition 1) or $f(\lambda; t_i) \equiv 0$

(condition 2). The **for** loop in the algorithm handles the special case in which a zero t_i of $\Delta_f(t)$ corresponds to when $f(\lambda; t_i) \equiv 0$. This may happen when the containing planes of both conics $\mathcal{A}(t_i)$ and $\mathcal{B}(t_i)$ are parallel so that $\mathcal{L}(u; t_i)$ is a line at infinity, and the conics are not in contact. The function $f(\lambda; t_i)$ may also be identically zero when $\mathcal{A}(t_i)$ and $\mathcal{B}(t_i)$ lie on the same plane so that $\mathcal{L}(u; t_i)$ becomes undefined. The two conics may or may not have a contact in this case and therefore we need to further carry out a 2D static collision detection of $\mathcal{A}'(t_i)$ and $\mathcal{B}'(t_i)$, the image of $\mathcal{A}(t_i)$ and $\mathcal{B}(t_i)$ under a rigid transformation to $\mathbb{R}^2$. The conics $\mathcal{A}(t_i)$ and $\mathcal{B}(t_i)$ are in contact if and only if the characteristic equation of $\mathcal{A}'(t_i)$ and $\mathcal{B}'(t_i)$ has a multiple root. In any case, a candidate contact time instant that corresponds to a contact point at infinity is discarded.

Algorithm 2. Computing the candidate time instants for two moving conics in $\mathbb{R}^3$

> **Input:** Two moving conics $\mathcal{A}(t)$ and $\mathcal{B}(t)$ defined in the planes $\Pi_A(t)$ and $\Pi_B(t)$ in $\mathbb{R}^3$, $t \in [t_0, t_1]$, respectively.
> **if** $\Pi_A(t) \equiv \Pi_B(t)$ for $t \in [t_0, t_1]$ **then**
>   Reduce CCD of $\mathcal{A}(t)$ and $\mathcal{B}(t)$ to that of two moving conics in a plane which is handled by Case VIII (Section 5.8)
> **else**
>   Compute the intersection line $\mathcal{L}(u; t)$ between $\Pi_A(t)$ and $\Pi_B(t)$
>   Compute $h(u; t)$ and $g(u; t)$ as in Eq. (2) and obtain $\widehat{A}(t)$ & $\widehat{B}(t)$ by rewriting $h(u; t) = U^T\widehat{A}(t)U$ and $g(u; t) = U^T\widehat{B}(t)U$ where $U = (u, 1)^T$
>   Compute $f(\lambda; t) = \det(\lambda\widehat{A}(t) - \widehat{B}(t))$ and the discriminant $\Delta_f(t)$ of $f(\lambda; t)$
>   **for all** $t_i \in \{t | \Delta_f(t) = 0\}$ **do**
>   **if** $\Pi_A(t_i) = \Pi_B(t_i)$ **then**
>   Transform $\mathcal{A}(t_i)$ and $\mathcal{B}(t_i)$ to $\mathcal{A}'(t_i)$ and $\mathcal{B}'(t_i)$ in $\mathbb{R}^2$
>   **if** the characteristic equation of $\mathcal{A}'(t_i)$ and $\mathcal{B}'(t_i)$ has a multiple root **then**
> $\mathcal{T} \leftarrow \mathcal{T} \cup \{t_i\}$
>   **else if** $\Pi_A(t_i)$ and $\Pi_B(t_i)$ are not parallel **then**
> $\mathcal{T} \leftarrow \mathcal{T} \cup \{t_i\}$
>   **return** $\mathcal{T}$ as the candidate contact time instants

5.8. Case VIII – conics vs. conics in $\mathbb{R}^2$

CCD of two conics in a plane is handled using the same algebraic approach as in [11] for CCD of two ellipses in $\mathbb{R}^2$. Given two moving conics $\mathcal{A}(t) : \overline{X}^T A(t)\overline{X} = 0$ and $\mathcal{B}(t) : \overline{X}^T B(t)\overline{X} = 0$ in $\mathbb{R}^2$, where $\overline{X} = (x, y, w)^T$ and $t \in [t_0, t_1]$, the characteristic equation $f(\lambda; t) = \det(\lambda A(t) - B(t)) = 0$ is cubic in λ. The equation $f(\lambda; t_0) = 0$ has a multiple root λ_0 if and only if $\mathcal{A}(t_0)$ and $\mathcal{B}(t_0)$ have tangential contact at time t_0. Hence, we compute the discriminant $\Delta_f(t)$ of $f(\lambda; t)$, and the zeroes of $\Delta_f(t)$ would be the candidate contact time instants of $\mathcal{A}(t)$ and $\mathcal{B}(t)$. For each contact time instant t_i, the contact point is given by the solution of $(\lambda_0 A(t) - B(t))\overline{X} = 0$ where λ_0 is a multiple root of $f(\lambda; t) = 0$.
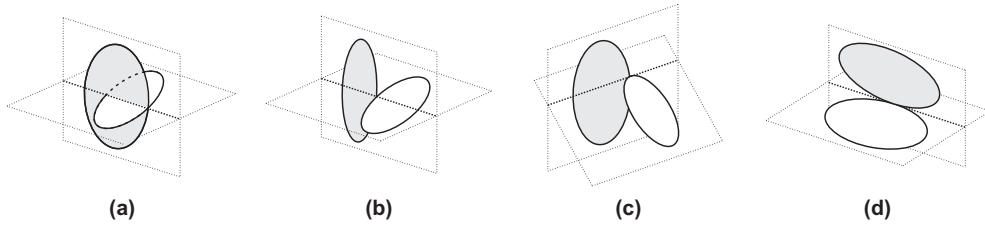
Fig. 8. The four configurations of two touching conics in 3D. Sub-figures (a), (b), (c) & (d) correspond to the cases (6), (7), (8) & (11) of Table 3, respectively.

5.9. Case IX – conics vs. lines in $\mathbb{R}^3$

Consider CCD between a conic $\mathcal{C}(t)$ and a line $\mathcal{L}(u;t)$ in $\mathbb{R}^3$. We assume that $\mathcal{C}(t)$ is given as the intersection between a quadric $\widehat{\mathcal{C}}(t) : X^T\widehat{C}(t)X = 0$ and a plane $\Pi_{\mathcal{C}(t)}$ in $\mathbb{R}^3$ (so that the axis of $\widehat{\mathcal{C}}(t)$ is orthogonal to $\Pi_{\mathcal{C}}(t)$). We may disregard the case of $\mathcal{L}(u;t)$ and $\Pi_{\mathcal{C}(t)}$ being always identical, as any possible first contact of the CQMs due to $\mathcal{C}(t)$ and $\mathcal{L}(u;t)$ can then be detected by CCD of $\mathcal{L}(u;t)$ and the neighboring boundary elements of $\mathcal{C}(t)$. If $\mathcal{L}(u;t)$ and $\Pi_{\mathcal{C}(t)}$ are parallel for all t, then $\mathcal{L}(u;t)$ and $\mathcal{C}(t)$ have no contact. Otherwise, we obtain $\mathbf{p}(t)$ which is the intersection of $\mathcal{L}(u;t)$ and $\Pi_{\mathcal{C}(t)}$. The conic $\mathcal{C}(t_i)$ is in contact with $\mathcal{L}(u;t_i)$ in $\mathbb{R}^3$ at time t_i if and only if $\mathbf{p}(t_i)$ lies on $\mathcal{C}(t_i)$, that is, $\mathbf{p}(t_i)^T\widehat{C}(t_i)\mathbf{p}(t_i) = 0$, and $\mathbf{p}(t_i)$ is not at infinity. Hence, the roots of $\mathbf{p}(t)^T\widehat{C}(t)\mathbf{p}(t) = 0$ are the candidate contact time instants; those of which corresponding to $\mathbf{p}(t_i)$ at infinity are discarded.

5.10. Case X – conics vs. lines in $\mathbb{R}^2$

Let $\mathcal{C}(t) : \overline{X}^T C(t)\overline{X} = 0$ be a conic and $\mathcal{L}(u;t)$ be a line in $\mathbb{R}^2$, where $\overline{X} = (x, y, w)^T \in \mathbb{PR}^2$. By substituting $\mathcal{L}(u;t)$ into $\mathcal{C}(t)$, we obtain $g(u;t) = L(u;t)^T C(t)L(u;t)$ which is quadratic in u. Each root t_i of the discriminant $\Delta_g(t)$ of $g(u;t)$ is a candidate contact time instant of $\mathcal{C}(t)$ and $\mathcal{L}(u;t)$, with a corresponding contact point $\mathcal{L}(u_0, t_i)$, where u_0 is a double root of $g(u;t_i)$.

5.11. Case XI – lines vs. lines

For CCD of two lines in $\mathbb{R}^3$, we seek the time instants at which the lines intersect in $\mathbb{R}^3$. Two lines $\mathcal{L}_1(u;t) = \mathbf{p}_1(t) + u\,\mathbf{q}_1(t)$ and $\mathcal{L}_2(v;t) = \mathbf{p}_2(t) + v\,\mathbf{q}_2(t)$ intersect in $\mathbb{PR}^3$ if and only if $\mathbf{q}_1(t), \mathbf{q}_2(t)$ and $\mathbf{p}_2(t) - \mathbf{p}_1(t)$ are coplanar. The contact time instants are then given by the roots of $g(t) = \det[\mathbf{q}_1(t), \mathbf{q}_2(t), \mathbf{p}_2(t) - \mathbf{p}_1(t)] = 0$. The case of $g(t) \equiv 0$ is neglected since it corresponds to two moving lines which are always coplanar; any contact between two moving line segments of this kind for two CQMs can be detected by CCD of an end vertex of one line segment and a CQM face on which the other line segment lies. For each candidate time instant t_0, the corresponding candidate contact point is given by $\mathbf{p} = \mathbf{p}_1(t_0) + u'\,\mathbf{q}_1(t_0)$, where $u' = ((\mathbf{p}_2(t_0) - \mathbf{p}_1(t_0)) \times \mathbf{q}_2(t_0)) \cdot (\mathbf{q}_1(t_0) \times \mathbf{q}_2(t_0))/|\mathbf{q}_1(t_0) \times \mathbf{q}_2(t_0)|^2$ (see [41]). The straight line $\mathcal{L}_1(u;t_0)$ and $\mathcal{L}_2(u;t_0)$ are parallel and have no contact in $\mathbb{R}^3$ if $|\mathbf{q}_1(t_0) \times \mathbf{q}_2(t_0)|^2 = 0$.

6. Contact validation

For each contact point computed from the CCD subproblems, we need to check if it is a valid contact point of two CQMs. A candidate contact point $\mathbf{p}$ is a valid contact point if and only if

1. $\mathbf{p}$ lies on both CQMs;
2. $\mathbf{p}$ constitutes an external contact of the CQMs, which means that the interior of the CQMs does not overlap.

We assume here that a CQM is obtained using CSG (constructive solid geometry). By recursive evaluation of the CSG construction trees, we can easily determine if a point lies on the surface of both CQMs or not. As for the second criteria, since the two given CQMs are separate initially, the first occurrence of a valid contact point must guarantee an external contact of the CQMs.

7. Two working examples

Example 7. In this example, we solve CCD of two moving capped elliptic cylinders $\mathcal{A}(t)$ and $\mathcal{B}(t)$, both are of the same size (Fig. 9a). The boundary elements of the cylinders are:

$$M_A(t) = \begin{pmatrix} 1 & 0 & 0 & -60t + 30 \\ 0 & 1 & 0 & 20 \\ 0 & 0 & 1 & 0 \\ 0 & 0 & 0 & 1 \end{pmatrix} \text{ and,}$$

$$M_B(t) = \begin{pmatrix} -2t^2 + 2t & 0 & -2t + 1 & -120t^3 + 180t^2 - 120t + 30 \\ 0 & 2t^2 - 2t + 1 & 0 & 160t^3 - 260t^2 + 180t - 50 \\ 2t - 1 & 0 & -2t^2 + 2t & 0 \\ 0 & 0 & 0 & 2t^2 - 2t + 1 \end{pmatrix},$$

- Face $F_{\mathcal{A},1}, F_{\mathcal{B},1}$: a cylinder $\frac{x^2}{5^2} + \frac{y^2}{10^2} = 1, z \in [-5, 5]$.
- Face $F_{\mathcal{A},2}, F_{\mathcal{B},2}$: a plane $z = -5$; and face $F_{\mathcal{A},3}, F_{\mathcal{B},3}$: a plane $z = 5$.
- Edge $E_{\mathcal{A},1}, E_{\mathcal{B},1}$: an ellipse $\frac{x^2}{5^2} + \frac{y^2}{10^2} = 1, z = -5$; and edge $E_{\mathcal{A},2}, E_{\mathcal{B},2}$: an ellipse $\frac{x^2}{5^2} + \frac{y^2}{10^2} = 1, z = 5$.

Cylinder $\mathcal{A}(t)$ assumes a linear translation, while cylinder $\mathcal{B}(t)$ assumes a degree-2 rotation as well as a linear translation. The motion matrices of $\mathcal{A}(t)$ and $\mathcal{B}(t)$ are respectively, $t \in [0, 1]$. We refer the readers to [36] for the details of the construction of the rational motion $M_B(t)$. The moving face $F_{\mathcal{A},1}$ can then be expressed as $X^T A(t) X = 0$, where $X = (x, y, z, 1)^T$ and $A(t) = M_A^{-T}(t) \, \text{diag}\left(\frac{1}{5^2}, \frac{1}{5^2}, 0, -1\right) M_A^{-1}(t)$. Expressions for other elements can be derived similarly by applying appropriate motion matrices.

The subproblems are listed as follows:

- $(F, F) - (F_{\mathcal{A},1}, F_{\mathcal{B},1})$
- $(F, E) - (F_{\mathcal{A},1}, E_{\mathcal{B},1}), (F_{\mathcal{A},1}, E_{\mathcal{B},2}), (F_{\mathcal{B},1}, E_{\mathcal{A},1}), (F_{\mathcal{B},1}, E_{\mathcal{A},2}), (F_{\mathcal{A},2}, E_{\mathcal{B},1}), (F_{\mathcal{A},2}, E_{\mathcal{B},2}), (F_{\mathcal{A},3}, E_{\mathcal{B},1}), (F_{\mathcal{A},3}, E_{\mathcal{B},2}), (F_{\mathcal{B},2}, E_{\mathcal{A},1}), (F_{\mathcal{B},2}, E_{\mathcal{A},2}), (F_{\mathcal{B},3}, E_{\mathcal{A},1}), (F_{\mathcal{B},3}, E_{\mathcal{A},2})$
- $(E, E) - (E_{\mathcal{A},1}, E_{\mathcal{B},1}), (E_{\mathcal{A},1}, E_{\mathcal{B},2}), (E_{\mathcal{A},2}, E_{\mathcal{B},1}), (E_{\mathcal{A},2}, E_{\mathcal{B},2})$

We shall show how four of the above CCD subproblems (corresponding to the four cases in Fig. 7) is solved. For brevity, contact point verification is skipped.

(F, F): $(F_{\mathcal{A},1}, F_{\mathcal{B},1})$—cylinder vs. cylinder

The characteristic polynomial $f(\lambda; t) = \det(\lambda A(t) - B(t))$ is quadratic in λ (since $\det(A(t)) \equiv 0$ and $\det(B(t)) \equiv 0$). The candidate time instants are the roots of $\text{Res}_\lambda(f, f_\lambda) = 0$, which are found to be $t_0 = 0.5, 0.625, 0.875$.

- For $t_0 = 0.5$, we have $f(\lambda; t_0) = 0$. The pencil $\lambda A(t_0) - B(t_0)$ is degenerate. Hence, we transform $\mathcal{A}(t_0)$ and $\mathcal{B}(t_0)$ by $M_A^{-1}(t_0)$ so that their axes (which are parallel) are orthogonal to the xy-plane, and check whether the cross-sectional ellipses on the xy-plane have any contact. Now, the characteristic polynomial $f(\lambda; t_0) = -(16\lambda - 1)(256\lambda^2 + 112\lambda + 1)$ of the cross-sec-

tional ellipses does not have any multiple root. Hence, there is no contact between the cylinders at $t = 0.5$.

- For $t_0 = 0.625, f(\lambda; t_0)$ has a multiple root and hence the cylinders are in contact. The contact point is found to be $(-7.5, 10, 0)^T$ and is verified to be a point on both capped cylinders. This is done exactly (see Remark 2). Therefore, a valid first contact at $t = 0.625$ is found for the cylinders. We may now skip the other larger roots of $\Delta_f(t) = 0$ and also other candidate time instants later than $t_0 = 0.625$ obtained in the subsequent CCD subproblems. (Note that in the followings, calculations for the later candidate time instant are still presented for illustrations, while they are skipped in practice for efficiency considerations.)

(F, E): $(F_{\mathcal{A},1}, E_{\mathcal{B},1})$—cylinder vs. ellipse

Both $F_{\mathcal{A},1}$ and $E_{\mathcal{B},1}$ are mapped by the same transformation such that $E_{\mathcal{B},1}$ is an ellipse in standard form on the xy-plane. The intersection of the transformed $F_{\mathcal{A},1}$ and the xy-plane is an ellipse $\mathcal{E}$, and CCD is performed between the two ellipses $\mathcal{E}$ and $E_{\mathcal{B},1}$. The characteristic polynomial of the ellipses are found to have a double root at $t_0 = 0, 0.6341, 1$.

- For $t_0 = 0, f(\lambda; t_0) = 0$ has a double root 0 which does not correspond to any valid contact and is hence rejected; $\mathcal{E}$ is indeed a line that does not touch $E_{\mathcal{B},1}$.
- For $t_0 = 0.6341, f(\lambda; t_0) = 0$ has a double root $\lambda_0 = -0.2843$. A single contact point $(-6.623, 10.414, -4.95)^T$ is found, which is verified to lie on both truncated cylinders.

(F, E): $(F_{\mathcal{A},3}, E_{\mathcal{B},1})$—plane vs. ellipse

Let $\mathcal{P}(t)$ be the plane $F_{\mathcal{A},3}$ and $\mathcal{E}(t)$ be the ellipse $E_{\mathcal{B},1}$. Both $\mathcal{P}(t)$ and $\mathcal{E}(t)$ are simultaneously transformed such that $\mathcal{E}(t)$ is in standard form on the xy-plane. The plane $\mathcal{P}(t)$ intersects the xy-plane in the line $\mathcal{L}(u; t) = (10t - 5, u(1 - 2t), 0, 4t^2 - 4t + 1)^T$. We now deal with CCD of the line $\mathcal{L}(u; t)$ and the ellipse
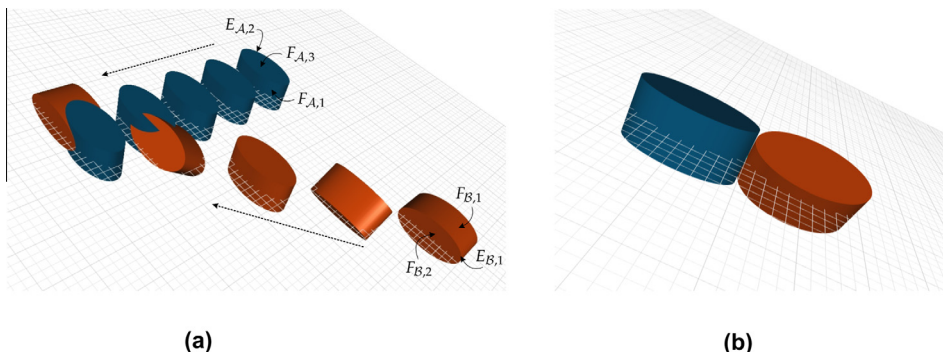

(a)

(b)

Fig. 9. (a) Two moving capped cylinders. (b) The cylinders are found to have the first contact at $t = 0.625$.
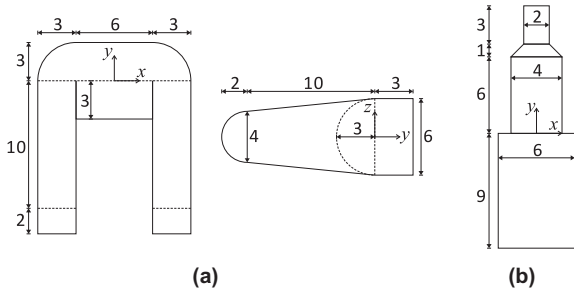
Fig. 10. Specifications of two CQM objects in Example 8.

$\mathcal{E}(t)$. Substituting $\mathcal{L}$ into the ellipse equation yields $h(u;t)$ and solving the discriminant $\Delta_h(t)$ gives the roots $t_0 = 0, 0.5, 1$.

- For $t_0 = 0$, solving $h(u;t_0) = 0$ gives $u_0 = 0$, and the contact point is given by $X_0 = (25, -50, 5)^T$. However, since $X_0^T E(t) X_0 = 49 > 0, X_0$ is not in the elliptic disk on $\mathcal{P}(t)$ and hence $t_0 = 0$ is rejected.
- For $t_0 = 0.5, \mathcal{P}(t_0)$ is parallel to the xy-plane, and t_0 is therefore rejected.
- For $t_0 = 1$, the contact point is found to be $X_0 = (-25, 30, 5)^T$ which does not lie within the elliptic disk on $\mathcal{P}(t)$ and $t_0 = 1$ is rejected.
- Hence, $\mathcal{P}(t_0)$ and $\mathcal{E}(t_0)$ are collision-free.

(E,E): $(E_{\mathcal{A},1}, E_{\mathcal{B},1})$—ellipse vs. ellipse

Let $\mathcal{E}_A(t)$ be $E_{\mathcal{A},1}$ and $\mathcal{E}_B(t)$ be $E_{\mathcal{B},1}$. We transform both ellipses simultaneously such that $\mathcal{E}_B(t)$ is in standard form on the xy-plane. The containing planes of the ellipses are not equal for all t and we proceed with CCD of two 1D ellipses, and the candidate contact times are $t_0 = 0.5, 0.6342, 0.875, 0.9658$.

- For $t_0 = 0.5, \mathcal{E}_A(t_0)$ lies on the xy-plane; hence, we perform collision detection for the two static ellipses $\mathcal{E}_1(t_0) : \frac{x^2}{25} - \frac{y^2}{100} - \frac{2y}{5} + 3 = 0$ and $\mathcal{E}_2(t_0) : \frac{x^2}{400} + \frac{y^2}{1600} + \frac{y}{80} = 0$. The characteristic equation for $\mathcal{E}_1(t_0)$ and $\mathcal{E}_2(t_0)$ has no multiple root, and hence there is no contact at $t_0 = 0.5$.
- For $t_0 = 0.6342$, the characteristic equation $f(\lambda)$ has a multiple root and the contact point is found to be $(-6.7084, 10.3668, -5)^T$.

Final result: Combining the results from all 17 subproblems, the two capped cylinders are found to have the first contact at $t = 0.625$ for the pair $(F_{\mathcal{A},1}, F_{\mathcal{B},1})$ at $(-7.5, 10, 0)^T$ (Fig. 9(b)). The algorithm is implemented with Maple using exact algebraic computations for all CCD formulations. We use floating point evaluation (15 significant digits) for solving the candidate time instants and computing the contact points. It takes 0.12 s to complete on an Intel Core 2 Duo E6600 2.40-GHz CPU (single-threaded).

$$M_B(t) = \begin{pmatrix} \begin{array}{l} \left(-u+1-1/\sqrt{2}\right)t^2 \\ +\left(u+\sqrt{2}\right)t \\ -1/\sqrt{2} \end{array} & \begin{array}{l} \left(1/\sqrt{2}-v\right)t^2 \\ +(v-\sqrt{2})t \\ +1/\sqrt{2} \end{array} & -vt^2+vt & \begin{array}{l} (-60u+120)t^3 \\ +(90u-180)t^2 \\ +(-30u+120)t-30 \end{array} \\ \begin{array}{l} \left(v-1/\sqrt{2}\right)t^2 \\ +\left(\sqrt{2}-v\right)t \\ -1/\sqrt{2} \end{array} & \begin{array}{l} \left(-u-1/\sqrt{2}\right)t^2 \\ +\left(u+\sqrt{2}\right)t \\ -1/\sqrt{2} \end{array} & \begin{array}{l} (1-u)t^2 \\ +ut \end{array} & \begin{array}{l} (9u-18)t^3 \\ +(16-8u)t^2 \\ +(-7-u)t-1 \end{array} \\ -vt^2+vt & \begin{array}{l} (u-1)t^2 \\ -ut \end{array} & \begin{array}{l} (1-u)t^2 \\ +(u-2)t \\ +1 \end{array} & \begin{array}{l} (20u-40)t^3 \\ +(60-30u)t^2 \\ +(-40+10u)t+10 \end{array} \\ 0 & 0 & 0 & \begin{array}{l} (2-u)t^2 \\ +(u-2)t+1 \end{array} \end{pmatrix},$$
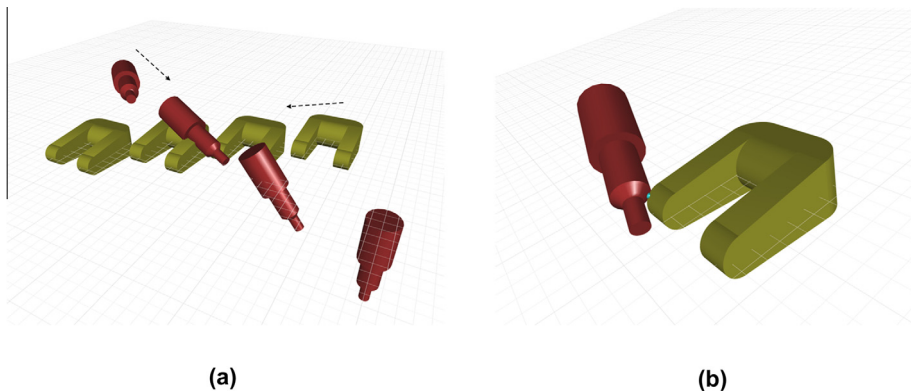

Fig. 11. (a) CCD of two CQMs in Example 8. (b) The first contact.

Example 8. In this example, we solve CCD for two moving CQMs as shown in Fig. 11(a). Object $\mathcal{A}$ comprises 45 boundary elements (4 cylinders, 9 planes, 10 circles, 14 lines and 8 vertices) while object $\mathcal{B}$ includes 13 boundary elements (3 cylinders, 1 cone, 3 planes and 6 circles). The specifications of the two objects are given in Fig. 10. Object $\mathcal{A}$ translates linearly on the plane while $\mathcal{B}$ moves with a linear translation and a degree-2 rotation (Fig. 11(a)). The motion matrices of $\mathcal{A}(t)$ and $\mathcal{B}(t)$ are

$$M_A(t) = \begin{pmatrix} 1 & 0 & 0 & 15-45t \\ 0 & 1 & 0 & 15-25t \\ 0 & 0 & 1 & 0 \\ 0 & 0 & 0 & 1 \end{pmatrix} \text{ and}$$

respectively, $t \in [0, 1]$. There are altogether 366 CCD sub-problems, and it takes about 5 s to complete the CCD computations under the same Maple environment as in Example 7. The first contact configuration is found to happen at $t = 0.313$ between the circle $\frac{(y+10)^2}{2^2} + \frac{z^2}{2^2} = 1, x = -6$, of $\mathcal{A}$ and the cone $x^2 + z^2 = (y-8)^2, y \in [6,7]$, of $\mathcal{B}$ as shown in Fig. 11(b).

8. Conclusion

We have presented a framework for CCD of composite quadric models (CQMs) whose boundary surfaces are defined by piecewise linear or quadric surface patches and whose boundary curves are conic curves or line segments. A hierarchy of CCD subproblems for various types of boundary element pairs in different dimensions are solved. Some subproblems can be solved using a dimension reduction technique so that the original problem is transformed to one in a lower dimensional space. In particular, we solved CCD of moving general quadrics and CCD of moving conics in $\mathbb{R}^3$. We also developed procedures for contact points verification to check if a contact point of the extended boundary elements lies on a CQM surface.

Our algorithm is exact in the sense that no approximation of the time domain or of the geometries is necessary. It only requires the evaluation of polynomial expressions at real roots of other univariate polynomials, the operations of which can be performed exactly (see Remark 2). Algebraic formulations are established for the CCD subproblems. Out of efficiency considerations, contact time instants and the corresponding contact points are solved for numerically. When the degree of motion is high, numerical stability problems thus introduced remain to be resolved.

In general, a boundary edge of a CQM may not be a conic curve, but rather a general degree four intersection curve of two boundary quadrics. Algorithms for CCD of this type of general CQMs still need to be developed. Major difficulties arise from the handling of degree four intersection curves. An idea is to reduce the problem of CCD of a moving general boundary edge and a moving quadric to the study of intersection of three quadrics in 3D (two of which intersect to give the boundary edge). There is a contact between a quadric surface $\mathcal{A}$ and a general boundary edge which is the intersection of two quadrics $\mathcal{B}$ and $\mathcal{C}$, if and

only if $\mathcal{A}, \mathcal{B}$ and $\mathcal{C}$ have a common singular intersection. The latter condition is indicated by that the quartic curve $G(\alpha, \beta, \gamma) \equiv \det(\alpha A + \beta B + \gamma C) = 0$ has a singular point. Hence, we need to develop methods to detect the time t_0 at which the moving planar quartic curve $G(\alpha, \beta, \gamma) = 0$ has a singular point. The case of CCD of two edges can be treated similarly, but is reduced to the study of the intersection of four quadrics, that is, the two pairs of quadrics defining two extended boundary curves. This will then lead to the study of singularity of a quartic surface.

References

[1] C. Ericson, Real-Time Collision Detection (The Morgan Kaufmann Series in Interactive 3-D Technology) (The Morgan Kaufmann Series in Interactive 3D Technology), Morgan Kaufmann Publishers Inc., San Francisco, CA, USA, 2004.

[2] P. Jiménez, F. Thomas, C. Torras, 3D collision detection: a survey, Comp. Graph. 25 (2) (2001) 269–285.

[3] S. Bischoff, L. Kobbelt, Ellipsoid decomposition of 3D-models, in: Proceedings of 1st International Symposium on 3D Data Processing, Visualization and Transmission (3DPVT 2002), Padova, Italy, June 19–21, 2002, pp. 480–488.

[4] D.-E. Hyun, S.-H. Yoon, M.-S. Kim, B. Jüttler, Modeling and deformation of arms and legs based on ellipsoidal sweeping, in: Proceedings of Pacific Graphics 2003, 2003, pp. 204–212.

[5] J. Canny, Collision detection for moving polyhedra, IEEE Trans. Patt. Anal. Mach. Intell. 8 (2) (1986) 200–209.

[6] E.G. Gilbert, D.W. Johnson, S.S. Keerthi, A fast procedure for computing the distance between objects in three-dimensional space, IEEE J. Robot. Automat. 4 (1988) 193–203.

[7] S. Gottschalk, M.C. Lin, D. Manocha, OBBTree: a hierarchical structure for rapid interference detection, in: SIGGRAPH, 1996, pp. 171–180.

[8] P.M. Hubbard, Approximating polyhedra with spheres for time-critical collision detection, ACM Trans. Graph. 15 (3) (1996) 179–210.

[9] X. Jia, W. Wang, Y.-K. Choi, B. Mourrain, C. Tu, Continuous Detection of the Variations of the Intersection Curves of Two Moving Quadrics in 3-Dimensional Projective Space, Tech. Rep. TR-2012-15, Department of Computer Science, The University of Hong Kong, 2012.

[10] S. Redon, A. Kheddar, S. Coquillart, An algebraic solution to the problem of collision detection for rigid polyhedral objects, in: Proceedings of the 2000 IEEE International Conference on Robotics and Automation, San Francisco, USA, 2000, pp. 3733–3738.

[11] Y.-K. Choi, W. Wang, Y. Liu, M.-S. Kim, Continuous collision detection for two moving elliptic disks, IEEE Trans. Robot. 22 (2) (2006) 213–224.

[12] Y.-K. Choi, J.-W. Chang, W. Wang, M.-S. Kim, G. Elber, Continuous collision detection for ellipsoids, IEEE Trans. Visual. Comp. Graph. 15 (2) (2009) 311–325.

[13] S. Cameron, Collision detection by four-dimensional intersection testing, IEEE Trans. Robot. Autom. 6 (3) (1990) 291–302.

[14] Y.J. Kim, S. Redon, M.C. Lin, D. Manocha, J. Templeman, Interactive continuous collision detection using swept volume for avatars, Presence 16 (2) (2007) 206–223.

[15] S. Redon, M.C. Lin, D. Manocha, Y.J. Kim, Fast continuous collision detection for articulated models, ASME J. Comput. Inform. Sci. Eng. 5 (2) (2005) 126–137.

[16] N.K. Govindaraju, I. Kabul, M.C. Lin, D. Manocha, Fast continuous collision detection among deformable models using graphics processors, Comp. Graph. 31 (1) (2007) 5–14.

[17] X. Zhang, S. Redon, M. Lee, Y.J. Kim, Continuous collision detection for articulated models using Taylor models and temporal culling, ACM Trans. Graph. 26 (3) (2007) 15.

[18] M. Tang, Y. Kim, D. Manocha, Continuous collision detection for non-rigid contact computations using local advancement, in: 2010 IEEE International Conference on Robotics and Automation (ICRA), 2010, pp. 4016–4021.

[19] T. Brochu, E. Edwards, R. Bridson, Efficient geometrically exact continuous collision detection, ACM Trans. Graph. 31 (4) (2012) 96:1–96:7.

[20] T.J.I. Bromwich, Quadratic forms and their classification by means of invariant-factors, Cambridge Tracts in Mathematics and Mathematical Physics, vol. 3, Hafner, New York, 1906.

[21] J. Semple, G. Kneebone, Algebraic Projective Geometry, Oxford University Press, London, 1952.

[22] M. Berger, Geometry, vol. II, Springer-Verlag, Berlin, 1987.

[23] W. Wang, Modelling and processing with quadric surfaces, in: M.K.G. Farin, J. Hoschek (Eds.), Handbook of Computer Aided Geometric Design, Elsevier, 2002, pp. 777–795.

[24] L. Dupont, Paramétrage quasi-optimal de l'intersection de deux quadriques: théorie, algorithme et implantation, Ph.D. thesis, Thèse d'université, Université Nancy II, 2004.

[25] L. Dupont, D. Lazard, S. Lazard, S. Petitjean, Near-optimal parameterization of the intersection of quadrics: I. The generic algorithm, J. Symb. Comput. 43 (3) (2008) 168–191.

[26] L. Dupont, D. Lazard, S. Lazard, S. Petitjean, Near-optimal parameterization of the intersection of quadrics: II. A classification of pencils, J. Symb. Comput. 43 (3) (2008) 192–215.

[27] L. Dupont, D. Lazard, S. Lazard, S. Petitjean, Near-optimal parameterization of the intersection of quadrics: III. Parameterizing singular intersections, J. Symb. Comput. 43 (3) (2008) 216–232.

[28] C. Tu, W. Wang, J. Wang, Classifying the nonsingular intersection curve of two quadric surfaces, in: Geometric Modeling and Processing (GMP 2002), Theory and Applications, Wako, Saitama, Japan, 2002, pp. 23–32.

[29] C. Tu, W. Wang, B. Mourrain, J. Wang, Using signature sequence to classify intersection curves of two quadrics, Comp. Aided Geomet. Des. 26 (3) (2009) 317–335.

[30] J. Levin, Mathematical models for determining the intersections of quadric surfaces, Comput. Graph. Image Process. 1 (1979) 73–87.

[31] J.R. Miller, Geometric approaches to nonplanar quadric surface intersection curves, ACM Trans. Graph. 6 (4) (1987) 274–307.

[32] I. Wilf, Y. Manor, Quadric-surface intersection curves: shape and structure, Comp.-Aid. Des. 25 (10) (1993) 633–643.

[33] W. Wang, B. Joe, R.N. Goldman, Computing quadric surface intersections based on an analysis of plane cubic curves, Graph. Mod. 64 (6) (2002) 335–367.

[34] W. Wang, R.N. Goldman, C. Tu, Enhancing levin's method for computing quadric-surface intersections, Comp. Aid. Geom. Des. 20 (7) (2003) 401–422.

[35] W. Wang, J. Wang, M.-S. Kim, An algebraic condition for the separation of two ellipsoids, Comput. Aid. Geom. Des. 18 (6) (2001) 531–539.

[36] B. Jüttler, M.G. Wagner, Kinematics and animation, in: M.K.G. Farin, J. Hoschek (Eds.), Handbook of Computer Aided Geometric Design, Elsevier, 2002, pp. 723–748.

[37] S. Basu, R. Pollack, M.-F. Roy, Algorithms in Real Algebraic Geometry (Algorithms and Computation in Mathematics), Springer-Verlag, New York, Inc., Secaucus, NJ, USA, 2006.

[38] Y.-K. Choi, W. Wang, B. Mourrain, C. Tu, X. Jia, F. Sun, Continuous collision detection for composite quadric models, 2013 <arXiv:1311.7462>.

[39] R.T. Farouki, C. Neff, M.A. O'Conner, Automatic parsing of degenerate quadric-surface intersections, ACM Trans. Graph. 8 (3) (1989) 174–203.

[40] Y.-K. Choi, Collision Detection for Ellipsoids and Other Quadrics, Ph.D. thesis, The University of Hong Kong, Pokfulam Road, Hong Kong, 2008.

[41] F.S. Hill Jr., The pleasures of "perp dot" products, Graph. gems IV (1994) 138–148.